





Article

The Design of Prometheus: A Reconfigurable UAV for Subterranean Mine Inspection

Liam Brown ^{1,*}, Robert Clarke ², Ali Akbari ³, Ujjar Bhandari ⁴, Sara Bernardini ³,
Puneet Chhabra ⁴, Ognjen Marjanovic ¹, Thomas Richardson ² and Simon Watson ^{1,*}

¹ Department of Electrical and Electronic Engineering, The University of Manchester, Manchester M13 9PL, UK; Ognjen.Marjanovic@manchester.ac.uk

² Department of Aerospace Engineering, University of Bristol, Bristol BS8 1TL, UK; robert.clarke@bristol.ac.uk (R.C.); thomas.richardson@bristol.ac.uk (T.R.)

³ Department of Computer Science, Royal Holloway University of London, London TW20 0EX, UK; Ali.Akbari@rhul.ac.uk (A.A.); sara.bernardini@rhul.ac.uk (S.B.)

⁴ Headlight AI Limited, London EC2A 1AF, UK; ujjar@headlight.ai (U.B.); puneet@headlight.ai (P.C.)

* Correspondence: liam.brown-2@manchester.ac.uk (L.B.); simon.watson@manchester.ac.uk (S.W.)

Received: 6 October 2020; Accepted: 12 November 2020; Published: 18 November 2020



Abstract: The inspection of legacy mine workings is a difficult, time consuming, costly task, as traditional methods require multiple boreholes to be drilled to allow sensors to be placed in the voids. Discrete sampling of the void from static locations also means that full coverage of the area cannot be achieved and occluded areas and side tunnels may not be fully mapped. The aim of the Prometheus project is to develop an autonomous robotic solution that is able to inspect the mine workings from a single borehole. This paper presents the challenges of operating autonomous aerial vehicles in such an environment, as well as physically entering the void with an autonomous robot. The paper address how some of these challenges can be overcome with bespoke design and intelligent controllers. It details the design of a reconfigurable UAV that is able to be deployed through a 150 mm borehole and unfold to a tip-to-tip diameter of 780 mm, allowing it to carry a payload suitable for a full autonomous mission.

Keywords: reconfigurable; UAS; drone; borehole; inspection; mines; folding

1. Introduction

There are thousands of miles of railway track and infrastructure spanning the UK. Due to the extent of the network and the scale of legacy mining activity in the UK, some railway infrastructure is in close vicinity to poorly mapped or unknown subterranean voids. Over 5000 of these voids are classed as ‘shallow’, meaning that if they were to collapse, it could cause movement on the surface. If this occurred near the railway, it may have a significant impact on the performance and safety of the network [1]. Due to this risk, old mine workings and other voids need to be regularly inspected to assess their stability and determine if and where any preemptive action needs to be taken. Figure 1 shows typical mellifluous mine workings.



Figure 1. Typical mellifluous mine workings.

Mine workings or voids of interest are currently inspected in three main ways:

1. If they are accessible and safe, the voids are entered by workers. Manual measurements and hand scanners are used to take surveys of the mines.
2. If they are accessible, but unsafe to enter by workers, remotely operated robotic systems can be used to build up geometric maps of the voids.
3. If they are inaccessible from the surface, boreholes are sunk into the workings and from them a picture of the void can be developed.

Out of the three methods, scanning via the borehole is the least effective as it can require many boreholes to scan the entire void. Drilling each borehole is costly, both financially and in time. It also limits the size of sensors that can be used, meaning bespoke costly LIDARs have to be used.

Due to the inefficiencies in this method, a system that is able to map the whole void from a single borehole would present significant savings in both time and cost of these inspections. This paper focuses on the design and development of such a system as part of the Prometheus Project.

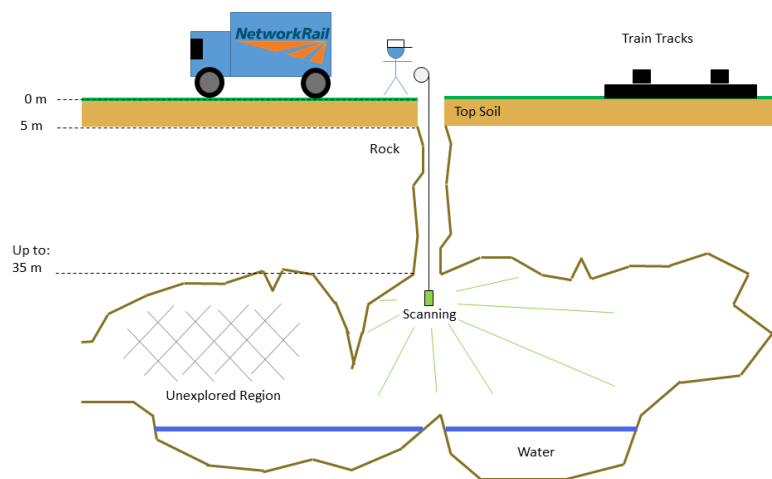
Prometheus (104824) is funded through the Industrial Strategy Challenge Fund under the Robotics and AI in Extreme Environments challenge. The Industrial Strategy Challenge Fund is delivered by UK Research and Innovation.

The project is partnering with Network Rail to propose a solution to the problem of mapping underground voids. Involving both academic and industrial partners, the project aim was to develop a borehole-deployed 'Unmanned Aerial System' (UAS) capable of autonomous, subterranean, 'Beyond Visual Line Of Sight' (BVLOS) exploration of the unknown voids, and producing a 3D map to allow the voids' risk to surface infrastructure to be assessed.

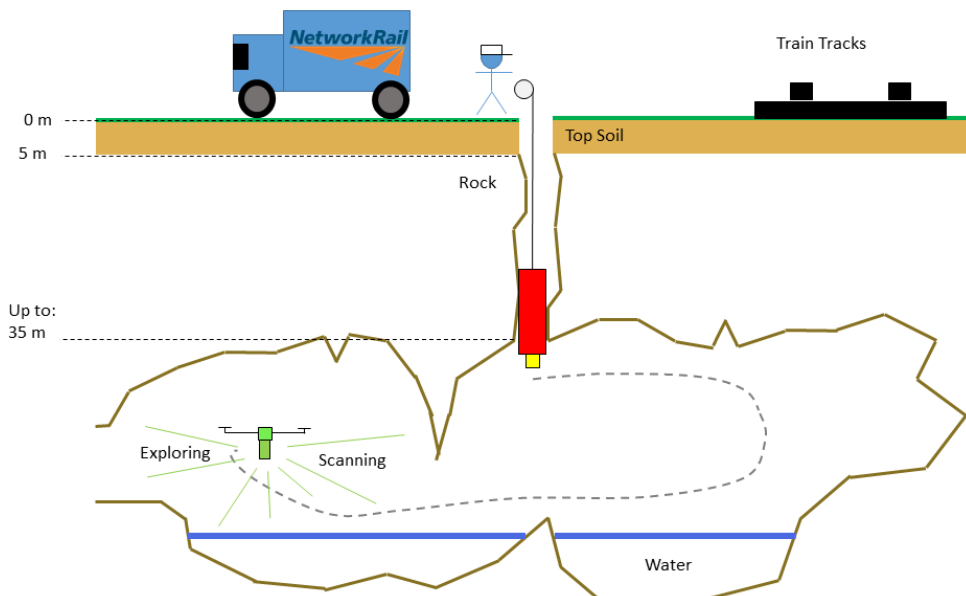
The benchmark for the required data is determined by reference to the GeoSLAM ZEB-REVO RT [2], a handheld scanner used in accessible mines. The scanner consists of a rotating Hokuyo LIDAR with custom software to stitch the data together. The ZEB-REVO RT is able to geometrically map voids with a relative accuracy of 1–3 cm depending on the environment.

1.1. Problem Definition

The problem discussed above as well as the proposed solution is represented in Figure 2. It can be seen in Figure 2a that there is an unexplored region, and multiple boreholes and scans are required to build up a complete map of the void. Whereas in Figure 2b, the robot is able to explore past the region within line-of-sight of the borehole and explore the entire void from a single borehole, saving both time and money.



(a) Traditional inaccessible void inspection



(b) Inaccessible void inspection with Prometheus

Figure 2. Problem definition.

1.2. Challenges of Borehole Inspection

There are a number of challenges that will be faced when operating in underground mine workings with the only access being through a borehole. This section provides an overview of some of these challenges and the derived requirements from them.

1.2.1. Size Constraints

There are two main factors which dictate size constraints for the system. The first is the borehole deployment. Theoretically, the access borehole could be drilled to any diameter required. However, increasing diameter comes with significant increases in cost and time required to sink the borehole. These increases may serve to offset the gains of a system capable of scanning away from the borehole entry. For this project, a nominal drill size of 150 mm was used, which also represents a typical access port size of many other installations. If lined or cased, the diameter is further reduced due to the thickness of the insert. Therefore, any system developed for mapping the voids must be able to fit down through this diameter.

The other main factor that applies to the system size is the system's ability to effectively explore beyond the entry point. Depending on the nature of the void, larger systems may be limited in their reach due to natural or man-made constrictions. A smaller system would be able to more extensively navigate the void system and present a more complete survey. For this project, the system design targets an overall bounding box of a 1 m³ cube.

1.2.2. Vertical Deployment

Due to the nature of the borehole access, the system is required to deploy from the roof of the void. It must therefore include a mechanism that is able to lower it into the void to allow it to start its mission. There are some inaccuracies in drilling the borehole so it is also required to be able to overcome small (<15°) deviations from the vertical.

1.2.3. Water

Active mines typically require constantly operating pumps to remove water from the workings. When mines are abandoned, they quickly flood, leading to large pools of standing water. This poses multiple challenges:

- A system may not be able to land or navigate on the floor if it is unable to float.
- The presence of water may add significant disturbances to sensors.

As well as underground pools, the voids may have running water through them, or water seeping from the ceiling. Due to this, the system must be water resistant. If there is no water present in the voids, they will likely be dusty. Taking the dust and water into account gives the requirement that the system must achieve an IP rating of IP62.

1.2.4. Hazardous Obstacles

Both natural and man-made voids present numerous obstacles, be they natural cave formations like stalactites, or abandoned mining infrastructure. These present navigation challenges to any vehicle. As well as the static obstacles, hanging tree roots and cables present dynamic obstacles, especially under the influence of vehicle induced air currents.

1.2.5. GPS Denied/Complex Workings

Commonly used satellite-based positioning systems such as GPS will not work underground. Therefore, the system must provide its own method of global position feedback. As well as being GPS denied, the mines are often dug to follow seams of minerals, this can mean that the shape of the workings are complex with lots of passages and turns. Therefore, when exploring the entire void, it is unlikely that any wireless link of sufficient bandwidth would be able to be maintained. This means the system needs to be capable of operating autonomously.

1.2.6. ATEX

Due to the potential for explosive atmospheres, the system is required to conform to the ATEX directives (Directive 99/92/EC and Directive 94/9/EC). These dictate specific safety standards that

anything entering a mine or other environment with potentially explosive atmosphere must obey. As this paper is presenting a prototype system, the design will only be ATEX sympathetic. This means it will not be fully compliant but no design decisions will be taken that will prevent future certification.

1.3. Paper Summary

This paper includes a review of the state of the art in robotic mine inspection as well as UASs capable of confined flight and active reconfiguration. Section 3 contains an overview of the proposed system to meet the challenges described in Section 1.2. Finally some initial results from the Prometheus project are shown and discussed in Section 4.

2. Literature Review

There are many robotics platforms that are currently used to reduce the need for the workers to enter unsafe mines, such as the Explora robot by ADR [3]. It is a wheeled robot that is able to overcome large obstacles and offer a stable platform for sensors. The platform itself contains no sensors, however additional sensing can be added depending on the required survey.

The use of robotics allows the automation of these inspection tasks, such as the development of a “6D SLAM” to navigate and map mines by Nuchter et al. [4]. Their large wheeled robot, the Groundhog, has a pair of laser ranger finders to develop 3D scans of a mine which are then matched to form a full scan. It is shown to successfully navigate and map a 250 m section of mine. Another mapping and navigation technique is developed with the Groundhog robot by Morris et al. [5]. This uses topological exploration, a topological planner, intersection detector and local navigator to plan the path of the robot with the primary focus being turning corners. From a practical experiment, they successfully turned 50 intersections, showing the method is successful, and generated point clouds of each intersection.

All of the discussed systems would be unable to be deployed for this application due to the inaccessible nature of the mine workings (Section 1.2.1) and the possibility of large bodies of water making ground-based robots unsuitable (Section 1.2.3). This leads to the use of a flying system such as the Onyxsrar Xena - LIDAR [6]. This system is able to fly over mine workings and map the surface, this can be very useful to survey open topped mines or monitor ground subsidence; however, the mines being targeted for the Prometheus system are enclosed and thus require a UAV that is able to fly in such an environment.

2.1. Confined Inspection UAS

Unmanned Aerial Systems (UASs) are being used for a variety of inspection and surveying tasks. This review will focus on those operating in confined environments including mines. One such system, developed by Castano et al. [7], flies through wet sewage pipes for visual inspection. It is ROS controlled and is able to be deployed from the roof. Nikolic et al. [8] developed a UAS for industrial inspection tasks in confined environments. They are able to navigate in confined GPS denied environments using only the inertial measurement unit and a pair of stereo cameras.

More robust designs, such as The Elios 2 [9] indoor inspection drone, use a caged design to protect the drone allowing it to contact surfaces without damaging the drone. This allows the drone to inspect confined spaces with a reduced risk of crashing. It has predominately manual control but with some autonomous features such as wall distance tracking. The Elios 2 is equipped with a camera for control and capturing data and uses photogrammetry on the captured images to produce 3D models. One major issue with a caged solution is the resulting twisting forces applied to the UAS when it comes into contact with an object, the Elios 1 [10] and the Droneball [11] avoids this major disturbance to the controller by mounting their drone on a gimbal inside the cage. This allows the cage to contact an obstacle and be rotated without affecting the pose of the drone. The other major shortcoming of the fully caged design is the increase in size of the robot. ADR offer drone inspection for mines [12]. Their Inspecta robot is a manually controlled octo-copter with guarded rotors and sensor package for

characterising mines, including cameras and LIDAR sensors for 3D mapping. Each propeller is encased in a caged sphere which helps to reduce the overall size of the robot but allows for propeller protection.

Inkonova offers two UASs that are able to complete autonomous 3D surveys in underground voids [13]. The two UASs are the Tilt Ranger and Scout, these use rotating 3D LIDARs to capture the geometric data from the void and perform collision avoidance with this data. Hovering Solutions [14] offer a similar solution, their Smart Flying Robot is able to autonomously navigate through underground voids and generate 3D maps of the environment. The Exyn A3R [15] is able to achieve an accuracy of <10 cm when developing 3D maps on an environment using a rotating Velodyne LiDAR Puck LITETM. It also is able to carry out autonomous confined missions. All the reviewed UASs are summarised in Table 1.

Table 1. Comparison of confined space Unmanned Aerial System (UAS) capabilities.

Capability Matrix			Specification				Capabilities					
			Nominal Weight	Tip to Tip Diameter	Flight Time	Photos	Video	Borehole Deployable	3D Reconstruction	Confined Autonomous Flight	Autonomous Exploration	
Robot			kg	mm	mins							
1	Flyability	Elios 2	1.45	400	10	Y	Y	N	Phgr	N	N	[9]
2	ADR	Inspecta	?	?	20	Y	Y	N	Y	N	N	[12]
3	Hovering Solutions	Smart Flying Robot	2	600	20	Y	Y	N	Y	Y	Y	[14]
4	Inkonova	Tilt Scout Tilt Ranger	?	?	15	?	?	N	Y	Y	Y	[13]
5	Exyn	A3R	?	1056.8	?	?	?	N	Y	Y	Y	[15]
6	Castano et al.	F450	?	704	?	Y	Y	N	N	Y	N	[7]
7	Prometheus	Titan-I	2.5	784.8	10	N	N	Y	Y	Y	Y	

Figure 3 shows the capabilities of some off the shelf UASs and those previously discussed in the literature. It can be seen that to be able to carry a payload that is able to perform autonomous exploration, a large UAS is required. Despite these systems offering the required 3D autonomous confined mapping, they are all too large to fit through a borehole (Section 1.2.1) and thus are unsuitable for this application. It can be seen from Figure 3 and Table 1 that the UASs that carry hardware for autonomous 3D navigation and mapping have larger diameters. This is due to the increased weight of the hardware, meaning more thrust is required to be generated and larger propellers (10–15 inch) are needed. A rigid UAS with large propellers will never fit through a 150 mm borehole, therefore a reconfigurable solution is required that can greatly reduce its diameter to fit through a borehole and then increase its size to accommodate large propellers when in the void. The target size and weight of the Prometheus prototype is also shown in Figure 3. This is at the low end of the size and weight scale compared to the other systems capable of operating autonomously, and offers a design that is borehole deployable.

2.2. Actively Reconfigurable UAS

Foldable or reconfigurable UASs are widely available in many commercial products such as the Go Pro Karma [16] and the DJI Mavic 2 [17]. They have this feature for storing them in smaller packages and making them easier to transport, meaning the user has to manually prepare the drone for flight. Due to the abundance of manually folded vehicles, only actively reconfigurable drones will be selected for review. The proposed system is required to unfold once it has passed through the borehole so manual operation would be unsuitable.

Flanaga et al. [18] has developed an actively reconfigurable quadrotor where each mounting arm for the propellers is controlled by a servo motor allowing all or any arm to be independently moved into H, T, X and O shapes or anything in between. They recalculate their centre of mass on the fly to allow the controller to adjust to the new configuration of the propellers.

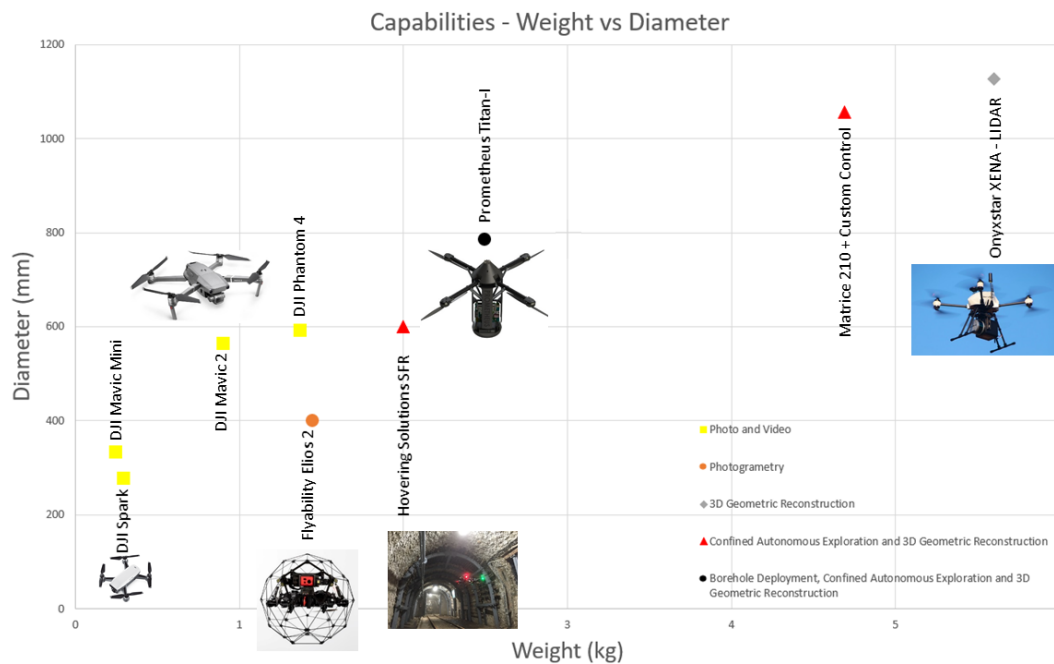


Figure 3. Weight and size of existing and proposed UAS.

Another quad rotor developed by Riviere et al. [19] uses an actuated elastic type mechanism to align the rotors into an almost straight configuration, reducing the wingspan by 48%. This is a very simple mechanism as it only requires a single actuator to rotate all four propellers, keeping the drone lightweight. There is a loss of roll control when it is in the folded state, thus it is only used to traverse small apertures not for a normal flight. Desbiez et al. [20] has developed the X-Morf, a similar system to align the rotors, by actuating the centre of the X shape of the quadrotor, it is able to reduce its wingspan by 28.5%.

Bucki and Mueller [21] developed a morphing quadrotor that uses passive springs to fold in the arms of the UAV when the propellers are not providing enough thrust to hold them out. This enables the UAV to fold to 50% of its diameter during flight and fit through confined spaces that the full sized robot could not. The unfolded system has a tip-to-tip diameter of 540 mm and a folded diameter of 280 mm.

Zhao et al. [22] uses a complex geometric expanding centre to alter the diameter of the robot and thus alter the X size of the UAS. The number of links in the body changes the amount the drone can expand and contract so it can be tailored to its application. They successfully completed flight tests with the deformation proving the feasibility of the system.

Zhao et al. have developed two multi-link drones [23,24]. The first multi-link multirotor is a snake link body with rotors on each of the four links, the links all actuate on the same plane meaning they can transform from a straight line to a circle (forming a normal quadrotor shape) [23]. Due to its movement, it is able to grip objects in the centre of the O shape, this grasping of objects is the primary focus of the paper. The DRAGON [24] is the second drone, again it is a snake link design but it has multiple degrees of freedom that allow it to have complex shapes when flying. A complex kinematic and dynamic model is required to help with the control system, it is shown to be able to fly but more challenging testing is yet to be completed. It has a total mass of 7 kg.

Other systems such as the TiltDrone developed by Zheng et al. [25] allow the body of the UAV to rotate in relation to the propellers to enable it to navigate narrow areas. They are able to achieve a 30 degree tilt in flight giving a 13.4% decrease in diameter.

The actively reconfigurable UASs discussed above are all aimed at modifying their shape during flight, and not designed to carry the payload required for fully autonomous exploration and flight. The Prometheus system is only required to reconfigure when being deployed or retrieved from the

void and does not need to fold during flight. Adding the ability to reconfigure during flight not only changes the dynamics of the system, likely making off the shelf flight controllers unsuitable, but also increases the weight of the UAS as it is carrying the additional actuation. Therefore, a unique solution is required.

This paper presents the development of the actively reconfigurable, borehole deployable, autonomous Titan-I prototype as part of the Prometheus project.

3. System Overview

This section describes the novel solution being developed to address the challenges highlighted in Section 1.2 and in the literature.

The proposed solution consists of three major sub-systems, as shown in the simplified system diagram (Figure 4). Prometheus is a multi-partner project, the areas each partner is working on are labelled on the diagram. The partners are as follows, Headlight AI (HAI), Thales (Th), Royal Holloway University of London (RHU), University of Bristol (UoB) and The University of Manchester (UoM). The partners not shown in the figure are Network Rail and Callen-Lenz.

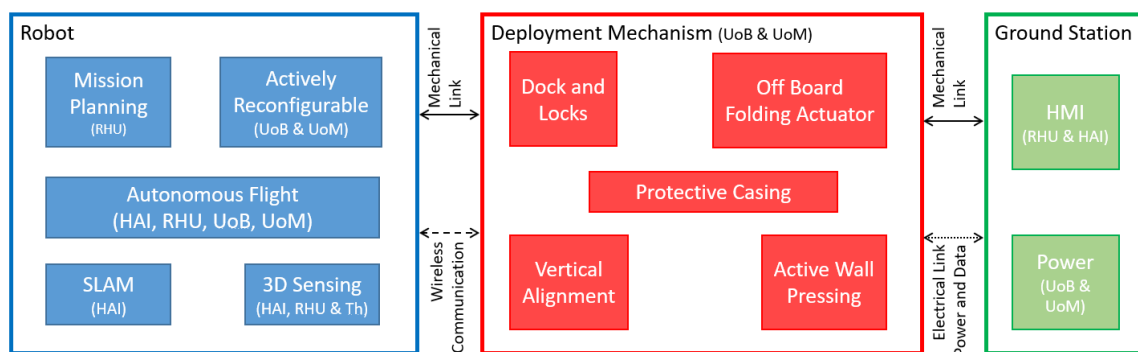


Figure 4. Simplified system diagram for Prometheus.

The three sub-systems are:

1. **'Ground Station' (GS)** (Figure 4, Green) provides the input and output of data from the rest of the system to the user ('Human Machine Interface' (HMI)). It is physically above ground and provides power and user input to the rest of the system.
2. **'Deployment Mechanism' (DM)** (Figure 4, Red) is responsible for deploying and extracting the robot from the surface and into the void through the borehole. It consists of a dock to allow the robot to detach and reattach to it at the start and end of the mission, respectively.
3. **Robot** (Figure 4, Blue) completes the survey. It is an autonomous inspection UAS that explores the mine workings and captures the required data product.

To be able to achieve the challenges highlighted in Section 1.2, some key design features have been developed. They are labelled in Figure 5 where the DM is shown in red and the robot in blue. Each sub system and feature are explained in more detail in the following sections.

3.1. Deployment Mechanism

This section presents the design features of the DM to make it suitable for operating in a mine environment.

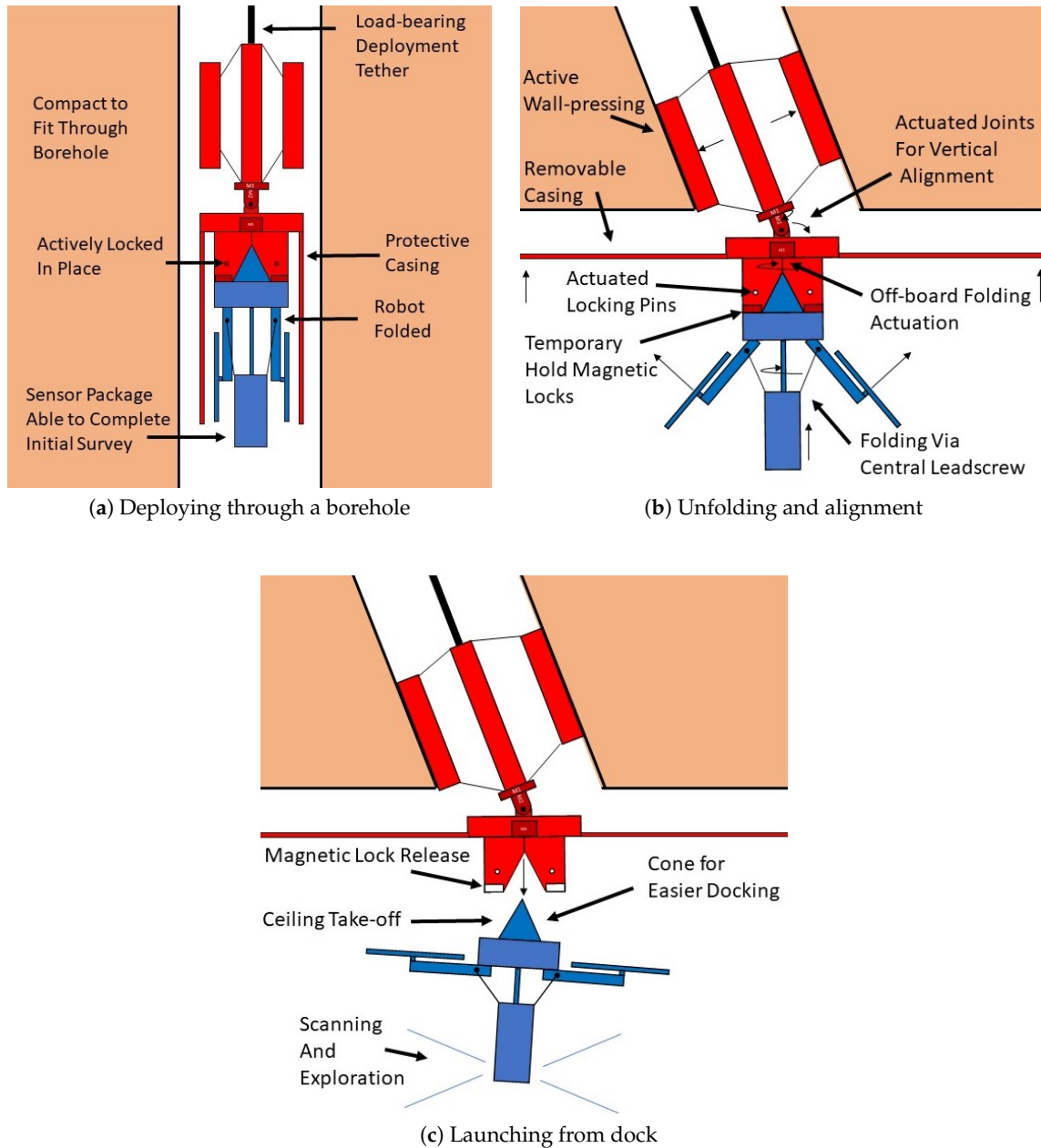


Figure 5. Key design features of the Deployment Mechanism and Robot.

3.1.1. Protective Casing

As discussed in Section 1.2.4, there can be rocks protruding into both the void and the borehole. To help protect the robot during deployment, a removable casing is placed around the robot to stop small pieces of debris from the drilling process damaging the robot. The casing provides a protective shield to the robot for the delicate electronics and flight hardware.

The casing is able to be folded out of the way once in the void to allow the robot to be unfolded and deployed. This is shown in Figure 5. The now exposed underside of the case is being used for a secondary purpose. It contains markers to assist in the return to home and docking of the robot at the end of the mission.

3.1.2. Off-Board Folding

Size constraints (Section 1.2.1) have a large impact on the design of the robot. To enable the robot to fit through the borehole, it is reconfigurable. To help maximise the payload capacity of the robot,

the primary actuator for the folding mechanism is placed off-board the robot on the DM. When docked, the motor is coupled to a central lead screw on the robot allowing it to be folded and unfolded at the start and end of the mission, respectively.

The 3D printed actuated lead screw is selected as it offers a lightweight, robust solution that is highly resistant to being backdriven, locking the arms in place during flight. The other considered options for actuation are:

1. Direct geared drive from off-board motor.
2. Individual actuation for each arm.

The major downfall with individual actuation is that it would require four motors to be mounted on-board the robot which would drastically increase the weight of the robot, this would have a negative impact on the flight time of the system. Direct geared drive offers an off-board driven, compact solution. However, the strength required for the gears significantly increases the folding mechanism mass.

3.1.3. Dock

As the robot enters the void from the roof, it is required to deploy from the ceiling (Section 1.2.2). A dock is required to hold the robot until it is ready to launch as well as provide an interface for the robot to be retrieved. The dock consists of two main sections, the robot side and the DM side. These are shown in Figure 6. It can be seen that the dock is a tapered cross shape. The taper provides passive alignment of the robot from an initial error of up to ± 20 mm. The cross shape provides torque transmission for the off-board folding motor and allows for more accurate geospatial alignment of the captured data.

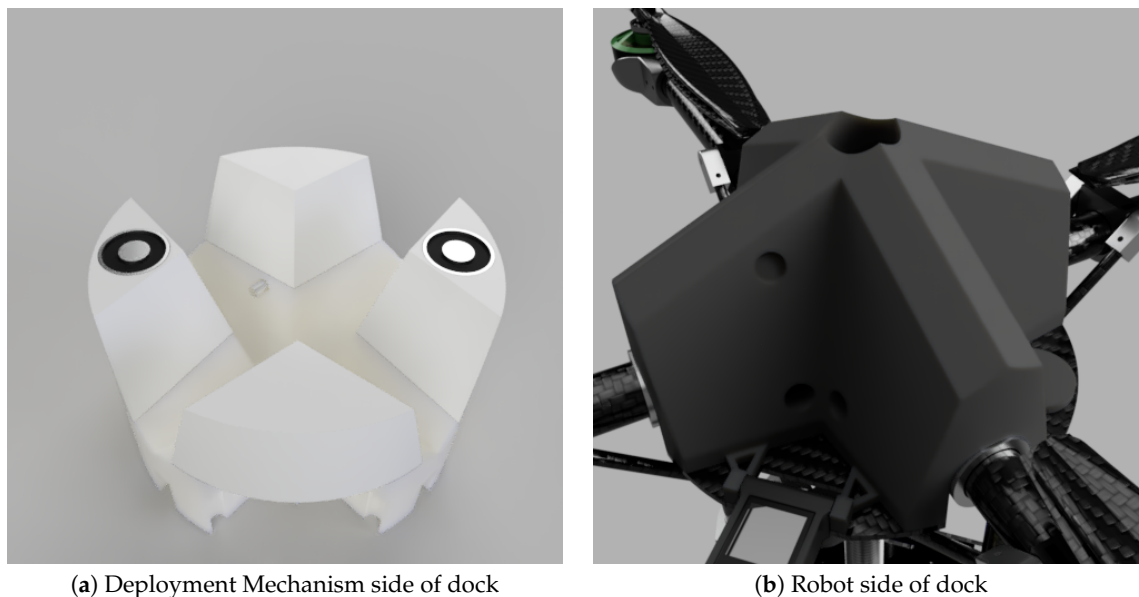


Figure 6. Dock design.

Prototypes of the docking interface have been constructed and tested in flight. A number of successful dock mating operations have been conducted; frames from the one such process can be seen in Figure 7. This testing was manually controlled with pilot visual reference. Work is ongoing to develop automated alignment and docking software. This utilises the existing vehicle sensors to generate alignment and ranging data.

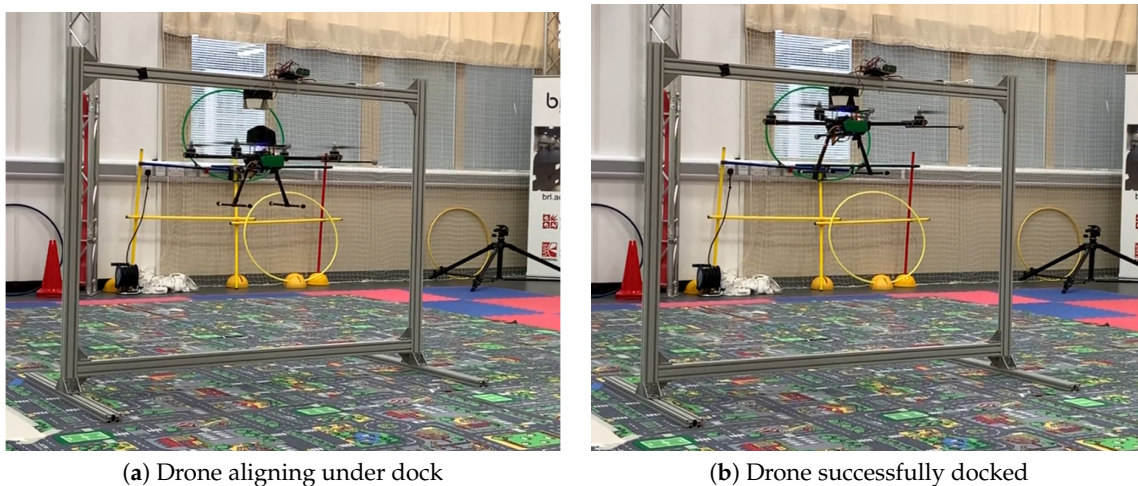


Figure 7. Drone mating successfully with dock from flight.

3.1.4. Locks

To safely hold the robot during borehole traversal and for vertical deployment (Section 1.2.2), locks are required to secure robot in the dock. The docking mechanism contains two stages of locks. The first stage consists of actuated locking pins, controlled by solenoids, which serve to latch the vehicle into the dock for safe traversal of the borehole. The second stage are magnetic locks, these act as a temporary holding mechanism just prior to departure, and immediately after docking. These are triggered to release when the vehicle has spooled up to estimated hover thrust and passively secure the vehicle when docking.

3.1.5. Active Wall-Pressing

To give safe and reliable release and docking of the robot to the DM, the dock is required to be stable and not move. To ensure this the DM utilises an active wall-pressing system to brace against the walls of the borehole. The mechanism is driven by a lead screw as it offers a compact design suitable to fit through the 150 mm borehole. Once braced against the walls of the borehole the DM can then align the dock to enable a safe launch.

3.1.6. Vertical Alignment

Due to the deviation in the borehole, the DM may not be vertical in the void (Section 1.2.2). For easier and safer launch and docking, the robot is aligned vertically. This is achieved by the alignment joint, which is actuated by two motors, one roll joint and one tilt. As well as aligning the robot vertically in the void, the joint also holds the combined system straight when in the borehole, limiting dragging along the borehole walls. For alignment, the gravity vector is found from an IMU and the motor angles are set using inverse kinematics as shown in Equations (1) and (2).

$$\theta_1 = \arctan \frac{G_x}{G_y}, \quad (1)$$

$$\theta_2 = \arctan \frac{G_{xy}}{G_z}, \quad (2)$$

where θ_1 and θ_2 are the alignment motor joint angles, G_x , G_y and G_z are the x , y and z components of the gravity vector, respectively and $G_{xy} = \sqrt{G_x^2 + G_y^2}$.

3.2. Robot

This section presents the design features of the robot that make it suitable for operating in a mine environment.

3.2.1. Reconfigurable Compact Design

To meet the size constraints dictated by the borehole diameter (Section 1.2.1), the robot is designed to be actively reconfigurable. When folded, the diameter of the robot is 130 mm, allowing for a protective casing to be placed around it and keeping the diameter below the required 150 mm to fit through the borehole.

Three deployment designs/strategies were considered:

1. Planar.
2. Aplanar arms-up.
3. Aplanar arms-down.

Planar folding describes a system where the motor arms fold in the same plane as the X of the vehicle as shown in Figure 8a. An example of planar folding is the UAS developed by Riviere et al. [19]. Aplanar is folding out of plane with the X, as shown in Figure 8b. Arms-up and arms-down describe the direction in which the arms fold, either from below the UAS or above it respectively. An example of this method of folding is shown on the Power Vision PowerEgg UAS [26].



Figure 8. Reconfigurable folding options.

In the planar strategy the folding mechanism is in a different plane to the thrust generated by the propellers of the motor meaning it will likely have the most rigid design, the can also have the most simple folding design only requiring one rotating joint. However, the folded package is very long, full tip-tip diameter of the robot, this makes traversing the borehole more difficult and deployment more complex as the UAS would need to be rotated through approximately 90° to be horizontal once in the void. The nature of this layout would also constrain the size of the payload significantly.

Aplanar arms-up and arms-down have some common benefits: if the payload is at the bottom of the robot the sensor package can be used to perform an initial survey of the void checking it is safe for deployment. Additionally, as the folded vehicle is delivered in the correct orientation for flight, no significant rotation is required for deployment. This also allows off-board actuation for the folding mechanism, reducing the weight. The folded package has a length around half the tip-tip diameter of the robot. However, it leads to a greater diameter robot and more complex folding mechanisms, usually a minimum of four rotating joints. Another disadvantage of the aplanar folding is that the folding direction is in the same plane as the thrust meaning it likely has a less rigid structure when comparing it to the the planar design. The arms-up folding (folded propellers point to the bottom of the robot) has some additional advantages over the arms-down (folded propellers point to the top of

the robot) design. The arms-up configuration folds in the opposite direction to thrust meaning bump stops or similar can be used to help increase the rigidity once unfolded.

The selected configuration is the aplanar arms-up folding design, this was selected due to the ease of deployment vs. the planar system and increased rigidity when compared to arms-down method.

The unfolded diameter of the system is 780 mm, approximately 6x larger than the folded diameter. This allows for 12 inch propellers to be fitted to the the UAS. In addition to changing diameter, the height of the robot reduces by 90 mm as it unfolds, which helps to increase the number of voids it can navigate through.

The overall size of the system does reduce the size of voids it can explore as it physically will be unable to fit through some passageways. However, it is still a major improvement over the current method of scanning from the end of a borehole. The reconfigurable design is only for the purpose of placing the robot into the void and will not be used during flight, it is to allow the system to fit through the 150 mm borehole (Section 1.2.1) and be able to carry the required payload for the full autonomous mission. Once in the void and unfolded, as shown in Figure 5, the arms are held in place by the lead screw and the actuation for the folding mechanism is left behind on the deployment mechanism (Section 3.1.2) so the robot is unable to reconfigure once undocked.

3.2.2. 3D Sensing and Mapping

The sensing is provided from a custom 360 degree 3D depth sensor package, Dragonfly. The Dragonfly has been developed by Headlight AI and outputs a ring of point cloud data from an array of IR cameras with a range of approximately 4 m. The field of view of the sensor is 360 degrees horizontally by 60 degrees vertically, it provides 344,736 points in each sample.

The robot uses 3D occupancy map information to localise itself and identify which areas are either free or occupied. The sensors publish a point cloud which is then fused and used to construct the 3D map. The 3D occupancy map classifies the robot's work space into free and collision space.

3.2.3. Autonomous Flight

Planning collision free paths is the key component of autonomous navigation. Motion planning deals with finding a collision-free path including a set of way-points. It is mostly done in the configuration space [27]. We developed a sampling-based motion planning algorithm which is able to plan under incomplete information about the free and occupied space of the robot's work space and has the re-planning capability. When the robot starts following the path, more information is captured through the sensors and is fed to planning. This allows the robot to evaluate whether the rest of way-points are collision-free or not in the path. If any collision is detected, the re-planning process is taking place that results in a new path from the current way-point. This allows the robot to navigate to new areas while preserving safety.

The planning is implemented on-board the robot, the proposed computing for the system is the Intel NUC NUC7i7DNKE. The robot will be controlled using the ROS framework [28].

3.2.4. Mission Planning

We developed a high-level planner to guide the robot exploration task [29]. The planner collects the frontier nodes, which are the ones located between known and unknown areas, using the information of the 3D occupancy map. It performs reasoning over the frontier nodes to choose the best one, and then triggers the autonomous navigation planner to find the path towards the chosen node from the current robot's state. In addition, the mission planner is able to accomplish a task using pre-scan data where the robot has complete knowledge about the environment.

4. Preliminary Confined Flight Testing

Due to the limitations caused by the Covid-19 pandemic, the practical development of the reconfigurable system has been delayed. Therefore, a set of experiments have been performed on

representative system and in simulation to determine the suitability of the proposed system. The three experiments are completed to test the integration of the software and flight hardware which will be used on the Prometheus robot. Section 4.1 describes the experimental set-up for the tests.

4.1. Experimental Setup

This section contains the description of three experiments, one confined flight, one autonomous planning and finally one flight based off the exploration and planning output. They are presented in Sections 4.1.1–4.1.3, respectively.

4.1.1. Confined Flight

The aim of the experiment was to test the integration of the on-board computing and flight system on a representative UAS. This will be testing three major components:

1. Test of flight controller in a confined environment.
2. Test of the injection of a positions from the main on-board PC through ROS.
3. Autonomous path tracking of the combined system in a confined environment.

To test the three parts, one experiment has been derived: to fly a pre-determine path in a confined basement. The on board sensing system will not be used to give position estimation but an external visual tracking system will be used for positioning feedback. This will be replaced by an on board localisation system once it is developed.

Figure 9 shows a confined basement with a VICON camera setup [30]. The VICON system is providing the visual feedback of position and pose to the flight controller through ROS.



Figure 9. Confined basement environment used for initial test flights.

A pre-scan of the environment was taken and stitched into a single cloud. This cloud is used to manually generate a safe path for the robot system to follow. Figure 10 shows the pre-scan of the environment, and the overlaid 'L' shaped path in yellow.

The path follows the waypoints in the following order, 1, 2, 1, 3, 1. The take off and landing both occur at waypoint 1.

The UAS being flown is representative of the final Prometheus robot, it uses the same autopilot, on-board PC and sensor package. During the flight, the 3D depth data from the sensor package are also recorded.

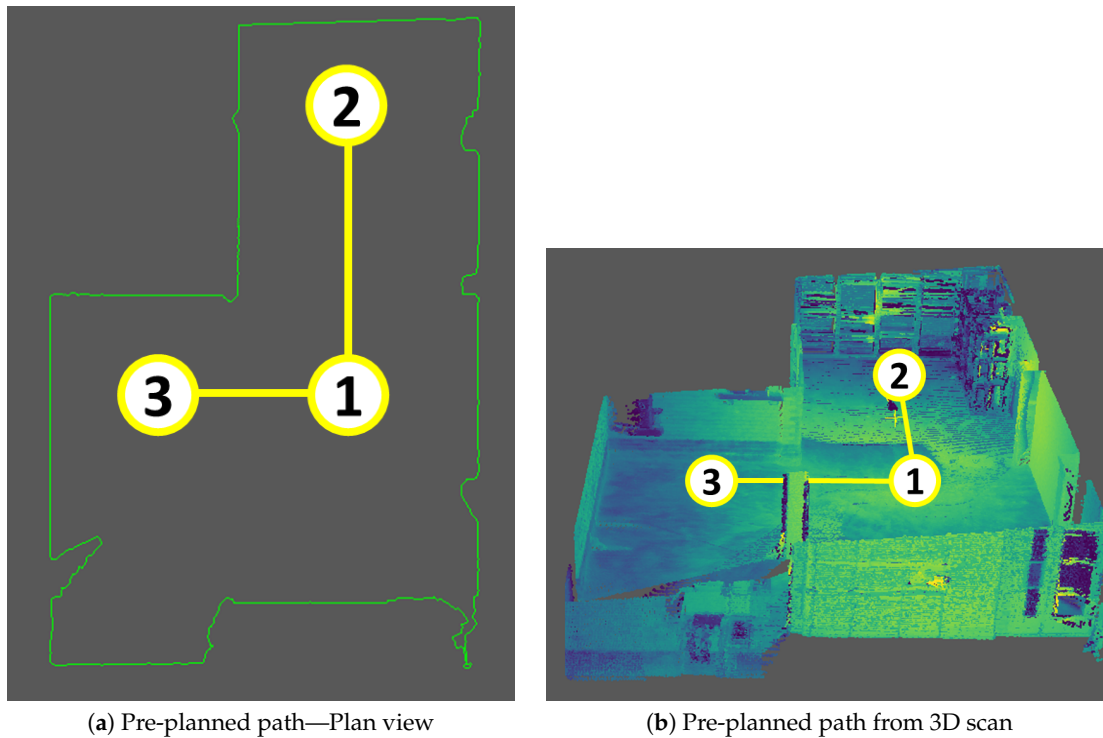


Figure 10. Pre-planned path overlaid on the processed 3D LIDAR data. (Processed by Headlight AI).

4.1.2. Autonomous Planning

The aim of this experiment was to test the proposed path planner on a pre-scan of the environment and determine if it generates a safe path for the robot.

This uses the same stitched point cloud of the environment from the previous experiment. A 3D occupancy map is constructed using the pre-scan which is made available to the mission planner. The planner is able to classify the map into free and collision space. The planner simulates the exportation with a model of the UAV. Using these components, the mission planner looks for collision-free paths. The paths are forwarded to the simulated robot's flight controller, and autonomous navigation is then carried out.

4.1.3. Autonomous Exploration and Planning Flight

The aim of this experiment was to generate an environment in a Gazebo simulation and run the exploration and planning algorithms to explore the area. Once the exploration is complete, the path will be taken out of the simulation and injected into the representative UAV and flown in a lab setting. This experiment tests the integration of the planning and exploration systems with the real world hardware of the UAV. The on-board sensors will not be used for localisation as an external VICON camera system will be used for positional information.

The generated environment is shown in Figure 11. It can be seen that there is a model of the reconfigurable robot in an void with a pillar in the centre.

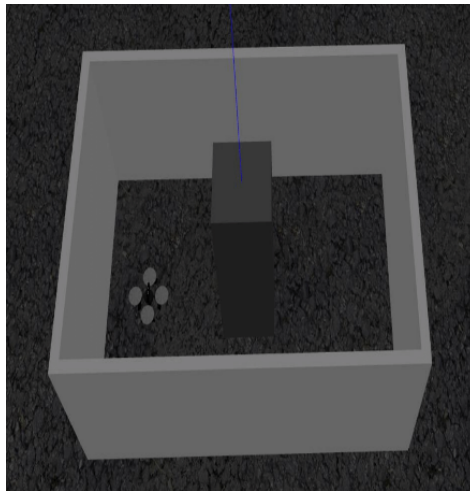


Figure 11. Robot in the simulation environment.

4.2. Results and Discussion

The results of the experiments are presented in the following section.

4.2.1. Confined Flight

Figure 12 shows a snapshot from the flight test. The full Video 1 can be found at <http://dx.doi.org/10.17632/65378d5s7n>. It can be seen that the UAS is successfully able to track the set points.



Figure 12. Snapshots of the confined flight.

The data gathered from the UAS are shown in Figure 13. These are the raw data from the 3D depth sensor package and key features of the environment (Figure 9) can be identified.

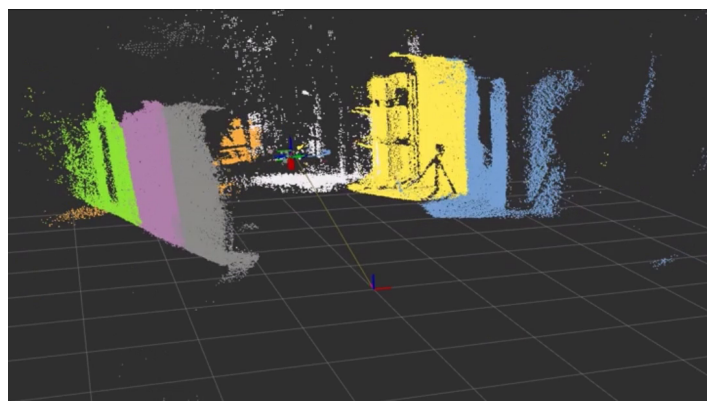


Figure 13. Example data from the Dragonfly sensor.

This successful flight shows the representative UAS successfully and autonomously navigating a manually generated pre-planned path. Not only does this show the success of the path tracking system but also confirms the integration of flight hardware and the interface of the on-board PC running ROS.

4.2.2. Autonomous Mission

The mission planner has been tested against the example represented in Figure 9. In this scenario, the task is to generate some collision-free paths using a pre-scan data. Figure 14 depicts the 3D occupancy map built using the fused point cloud. In this case, the planner has complete information about the environment and is able to obtain collision-free paths. Figure 15 indicates the set of “L” shaped paths which have to be followed by the robot. Figure 10 sketches the order of the paths in execution.

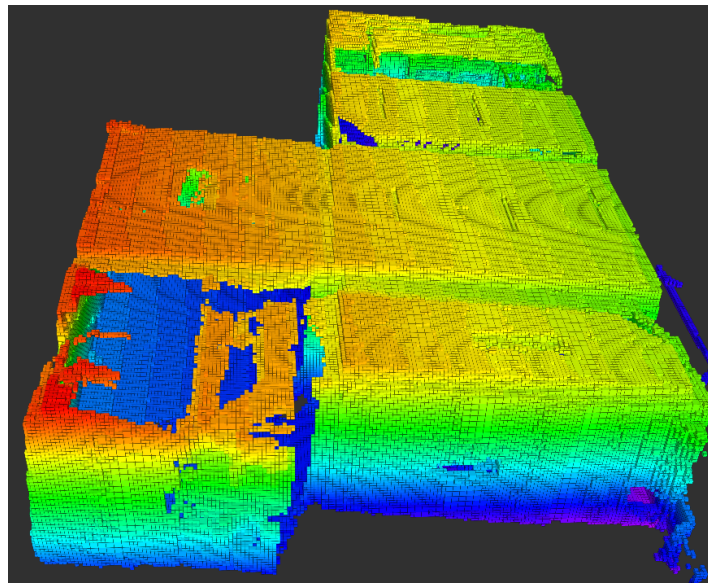


Figure 14. The 3D occupancy map based on the fused point cloud.

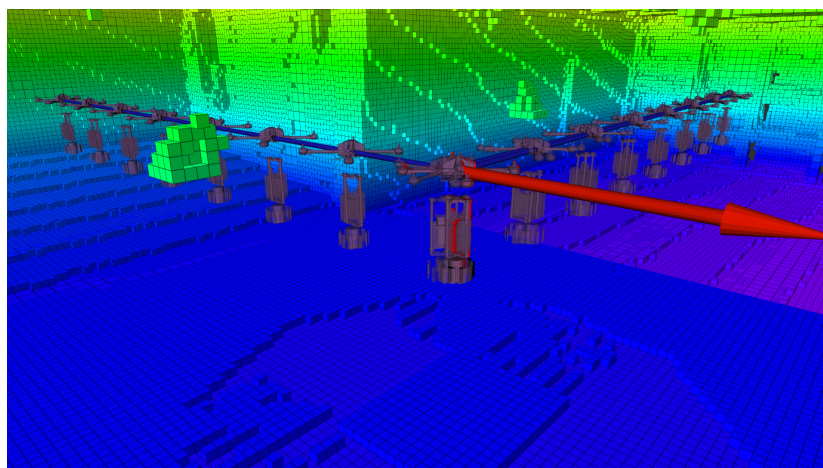


Figure 15. The “L” shaped path generated by the mission planner.

4.2.3. Autonomous Exploration and Planning Flight

The first stage of this experiment is the simulation of the exploration of the environment shown in Figure 11. This is completed successfully and snapshots of the exploration are shown in Figure 16.

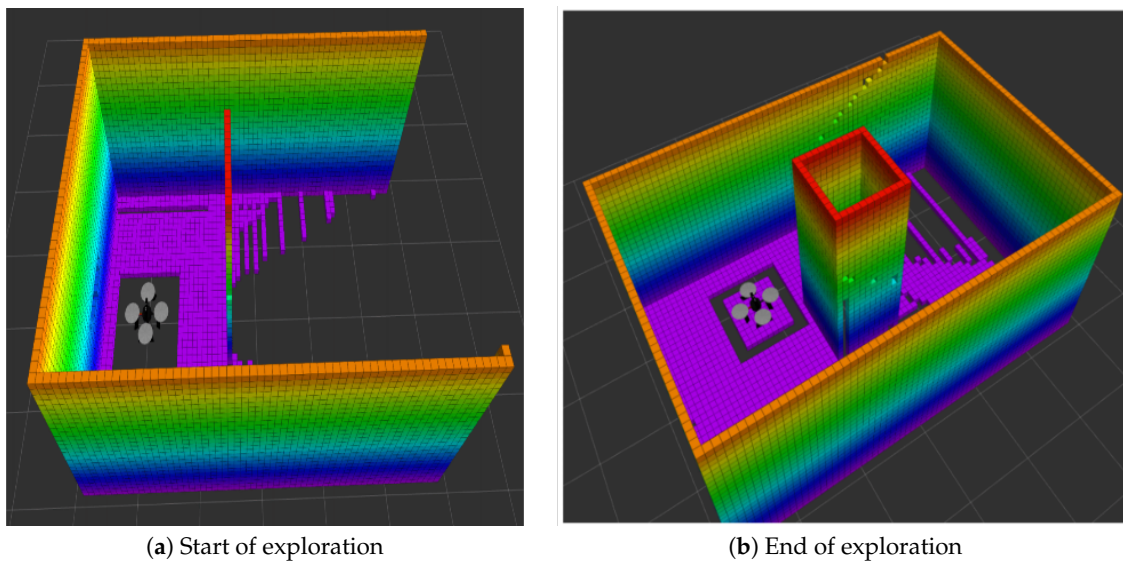


Figure 16. Snapshot of simulated exploration.

The Figure 16 shows two stages of the exploration, the first is the start of the mission where there are large areas on the void unknown to the robot, as shown as the areas with no colour in Figure 16a. Figure 16b shows the end of the mission where all the information that the robot is able to gather is known. This shows that the exploring is successful. The path flow in the simulation is shown in Figure 17.

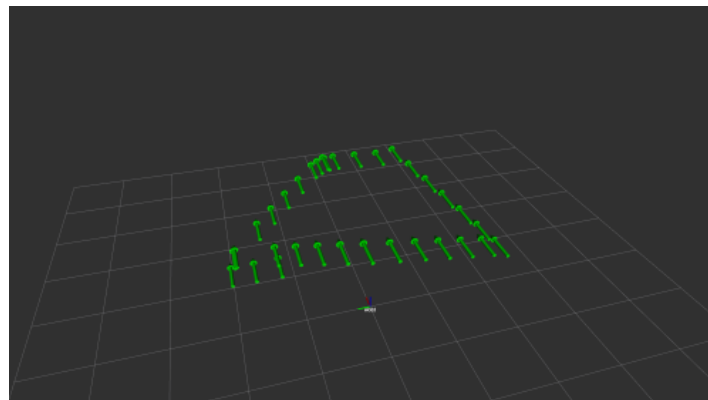


Figure 17. Flown path of the robot using the simulated exploration algorithms.

The path is two sweeping arches around the centre pillar with an elevation gain when it is alongside it. The path is then injected onto a real system as is successfully flow by the representative vehicle. The video of this is shown in Video 2, available at <http://dx.doi.org/10.17632/65378d5s7n>.

4.2.4. Discussion

Experiment 1—confined flight, shows the UAS successfully achieving the three targets for the experiment:

1. The robot was able to safely follow the pre-planned path in the confined environment, Video 1 shows small disturbances as the UAS was effected by ground effect but improved tuning of the flight controller should be able to reduce that effect.
2. As shown by successfully completing a safe flight, the position feedback from the VICON system was able to be injected into the flight controller through the ROS framework. Demonstrating that this works when in a region without external position feedback, the position reference will be generated from the on-board SLAM system which is still in development.

3. As shown in Video 1, the robot was able to safely and autonomously track the path. Future work would be the development of the path tracking to enable smoother transmissions between way points.

Experiment 2—autonomous mission, validates the safety of the proposed path planner. It shows that using the same data set as the manual path, that the planner is able to generate a safe path for the robot to follow that is comparable to the human made path. This shows that the planner is able to achieve a collision free path for the robot in a confined environment. The planner was able to generate this path based off the real world data in the simulated environment. Future aims of the project will be to execute the planning and exploration on the robot in real time.

Experiment 3—autonomous exploration and planning flight, shows the successful integration of the exploration and planning algorithms with the real world hardware of the robot. It showed a second scenario where the planner is able to generate a safe path for the robot and that this path is suitable for flight on a real world system.

Further areas of work on the project are integration of the real world dock and deployment mechanism with the exploration and planning algorithms, and the development of the localisation system using the on board sensors to remove the need for the external positioning systems used in this paper.

5. Conclusions

This paper proposes a solution to some of the challenges of operating in an unknown, subterranean mine environment. It demonstrates the integration of the selected flight hardware and autonomous planning and exploration. The presented results show a successful confined flight and a safe path generated by the planner. This is integrated and tested on a representative system to the final folding prototype. The future work for the Prometheus project is the construction and testing of the reconfigurable system as well as the implementation and development of the path planning algorithms.

Author Contributions: A.A., L.B., U.B. and R.C. contributed in Data curation, Formal analysis, Investigation, Methodology, Writing—original draft preparation, Writing—review and editing, Software and Validation. S.B., O.M., T.R. and S.W. contributed in Funding acquisition, Methodology, Writing—review and editing and Supervision. P.C. contributed in Data curation, Formal analysis, Funding acquisition, Investigation, Methodology, Writing—review and editing, Software, Supervision and Validation. All authors have read and agreed to the published version of the manuscript.

Funding: Prometheus (104824) is funded through the Industrial Strategy Challenge Fund under the Robotics and AI in Extreme Environments challenge. The Industrial Strategy Challenge Fund is delivered by UK Research and Innovation.

Acknowledgments: This work has been completed in partnership with the following companies who have provided insight and technical expertise to the project: Callen-Lenz, Headlight AI Limited, Network Rail Infrastructure Limited and Thales UK Limited.

Conflicts of Interest: The authors declare no conflict of interest.

References

1. Rail, N. Challenge Statement—Mining Ground Investigations. Technical Report, 2019. Available online: <https://www.networkrail.co.uk/wp-content/uploads/2019/06/Mining-Mining-Ground-Investigations.pdf> (accessed on 6 October 2020).
2. GeoSLAM. ZEB Revo RT. Available online: <https://geoslam.com/solutions/zeb-revo-rt/> (accessed on 19 May 2020).
3. Australian Droid + Robot. Explora S Package—Australian Droid + Robot. Available online: <https://www.australiandroid.com.au/collections/underground-inspection-mapping/products/explora-s-package> (accessed on 6 October 2020).
4. Nuchter, A.; Surmann, H.; Lingemann, K.; Hertzberg, J.; Thrun, S. 6D SLAM with an application in autonomous mine mapping. *Int. Conf. Robot. Autom.* **2004**, *2*, 1998–2003. [[CrossRef](#)]

5. Morris, A.; Silver, D.; Ferguson, D.; Thayer, S. Towards topological exploration of abandoned mines. *Proc. IEEE Int. Conf. Robot. Autom.* **2005**, *2005*, 2117–2123. [[CrossRef](#)]
6. OnyxStar. LIDAR Scanning - Aerial Laser Scanning by Drone. Available online: <https://www.onyxstar.net/lidar-scanning-aerial-laser-scanning-by-drone/> (accessed on 6 October 2020).
7. Castaño, A.R.; Romero, H.; Capitán, J.; Andrade, J.L.; Ollero, A. Development of a Semi-autonomous Aerial Vehicle for Sewerage Inspection. In *Robot 2019: Fourth Iberian Robotics Conference*; Silva, M.F., Luís Lima, J., Reis, L.P., Sanfeliu, A., Tardioli, D., Eds.; Springer International Publishing: Cham, The Netherlands, 2020; pp. 75–86.
8. Nikolic, J.; Burri, M.; Rehder, J.; Leutenegger, S.; Huerzeler, C.; Siegwart, R. A UAV system for inspection of industrial facilities. *IEEE Aeros. Conf. Proc.* **2013**. [[CrossRef](#)]
9. Flyability. Elios 2 - Indoor drone for confined space inspections. Available online: <https://www.flyability.com/elios-2> (accessed on 13 November 2020).
10. Flyability. Elios - Inspect & Explore Indoor and Confined Spaces. Available online: <https://www.flyability.com/elios/> (accessed on 13 November 2020).
11. Andrew Macdonald. Droneball The Collision Tolerant Drone | Indiegogo. Available online: https://www.indiegogo.com/projects/droneball-the-collision-tolerant-drone# (accessed on 13 November 2020).
12. Australian Droid + Robot. Inspecta Mine Inspection Drone Package—Australian Droid + Robot. Available online: <https://australiandroid.com/products/inspecta-mine-inspection-drone-package> (accessed on 13 November 2020).
13. INKONOVA. Available online: <https://www.inkonova.se/> (accessed on 19 May 2020).
14. Hovering Solutions. Flying Underground: The Use of Smart Flying Robots in Underground Mining. Available online: <http://www.hoveringsolutions.com/es/casos-de-estudio/underground-mining-flying-robots> (accessed on 19 May 2020).
15. Exyn. Available online: <https://www.exyn.com/mining/> (accessed on 18 May 2020).
16. Go Pro. Karma with HERO6 Black. Available online: <https://shop.gopro.com/EMEA/accessories-2/karma-with-hero6-black/QKWXX-601-EU.html> (accessed on 8 May 2020).
17. DJI. Mavic 2 - the Flagship Consumer Drone from DJI. Available online: <https://store.dji.com/product/mavic-2> (accessed on 8 May 2020).
18. Falanga, D.; Kleber, K.; Mintchev, S.; Floreano, D.; Scaramuzza, D. The Foldable Drone: A Morphing Quadrotor That Can Squeeze and Fly. *IEEE Robot. Autom. Lett.* **2018**, *4*, 209–216. [[CrossRef](#)]
19. Riviere, V.; Manecy, A.; Viollet, S. Agile Robotic Fliers: A Morphing-Based Approach. *Soft Robot.* **2018**, *5*, 541–553. [[CrossRef](#)] [[PubMed](#)]
20. Desbiez, A.; Expert, F.; Boyron, M.; Diperi, J.; Viollet, S.; Ruffier, F.; Desbiez, A.; Expert, F.; Boyron, M.; Diperi, J.; et al. X-Morf: A crash-separable quadrotor that morfs its X-geometry in flight. In Proceedings of the 2017 Workshop on Research, Education and Development of Unmanned Aerial Systems (RED-UAS), Linköping, Sweden, 3–5 October 2017.
21. Bucki, N.; Mueller, M.W. Design and Control of a Passively Morphing Quadcopter. In Proceedings of the 2019 International Conference on Robotics and Automation (ICRA), Montreal, QC, Canada, 20–24 May 2019.
22. Zhao, N.; Luo, Y.; Deng, H.; Shen, Y. The deformable quad-rotor: Design, kinematics and dynamics characterization, and flight performance validation. *IEEE Int. Conf. Intell. Robot. Syst.* **2017**, 2391–2396. [[CrossRef](#)]
23. Zhao, M.; Kawasaki, K.; Chen, X.; Noda, S.; Okada, K.; Inaba, M. Whole-body aerial manipulation by transformable multirotor with two-dimensional multilinks. *Proc. IEEE Int. Conf. Robot. Autom.* **2017**, 5175–5182. [[CrossRef](#)]
24. Zhao, M.; Anzai, T.; Shi, F.; Chen, X.; Okada, K.; Inaba, M. Design, Modeling, and Control of an Aerial Robot DRAGON: A Dual-Rotor-Embedded Multilink Robot with the Ability of Multi-Degree-of-Freedom Aerial Transformation. *IEEE Robot. Autom. Lett.* **2018**, *3*, 1176–1183. [[CrossRef](#)]
25. Zheng, P.; Tan, X.; Kocer, B.B.; Yang, E.; Kovac, M. TiltDrone: A Fully-Actuated Tilting Quadrotor Platform. *IEEE Robot. Autom. Lett.* **2020**, *5*, 6845–6852. [[CrossRef](#)]
26. Power Vision. PowerEgg - PowerVision | European. Available online: <https://www.powervision.me/eu/product/poweregg> (accessed on 13 November 2020).
27. Lozano-Pérez, T. Spatial Planning: A Configuration Space Approach. In *Autonomous Robot Vehicles*; Springer: New York, NY, USA, 1990; pp. 259–271. [[CrossRef](#)]

28. Quigley, M.; Gerkey, B.; Conley, K.; Faust, J.; Foote, T.; Leibs, J.; Berger, E.; Wheeler, R.; Ng, A. *ROS: An Open-Source Robot Operating System*; Technical Report; Willow Garage: Menlo Park, CA, USA, 2009.
29. Akbari, A.; Chhabra, P.; Bhandari, U.; Bernardini, S. Intelligent Exploration and Autonomous Navigation in Confined Spaces. In Proceedings of the 2020 IEEE/RSJ International Conference on Intelligent Robots and Systems (IROS), Las Vegas, NV, USA, 25–29 October 2020.
30. VICON. Motion Capture Systems. Available online: <https://www.vicon.com/about-us/> (accessed on 18 May 2020).

Publisher’s Note: MDPI stays neutral with regard to jurisdictional claims in published maps and institutional affiliations.



© 2020 by the authors. Licensee MDPI, Basel, Switzerland. This article is an open access article distributed under the terms and conditions of the Creative Commons Attribution (CC BY) license (<http://creativecommons.org/licenses/by/4.0/>).